Liquid Crystals
Publication details, including instructions for authors and subscription information:
http://www.informaworld.com/smpp/title~content=t713926090

Synthesis, liquid crystalline properties and fluorescence of polycatenar 1,3,4-oxadiazole derivatives

Haitao Wang[a]; Fenglong Zhang[a]; Binglian Bai[a]; Peng Zhang[a]; Jianhua Shi[a]; Dingyi Yu[b]; Yunfeng Zhao[b]; Yue Wang[b]; Min Li[a]
[a] Key Laboratory of Automobile Materials (MOE) & College of Materials Science and Engineering, Jilin University, Changchun, People's Republic of China [b] State Key Laboratory for Supramolecular Structure and Materials & College of Chemistry, Jilin University, Changchun, People's Republic of China

To cite this Article Wang, Haitao , Zhang, Fenglong , Bai, Binglian , Zhang, Peng , Shi, Jianhua , Yu, Dingyi , Zhao, Yunfeng , Wang, Yue and Li, Min(2008) 'Synthesis, liquid crystalline properties and fluorescence of polycatenar 1,3,4-oxadiazole derivatives', Liquid Crystals, 35: 8, 905 — 912
To link to this Article: DOI: 10.1080/02678290802262737
URL: http://dx.doi.org/10.1080/02678290802262737

Liquid Crystals,
Vol. 35, No. 8, August 2008, 905–912

Taylor & Francis
Taylor & Francis Group

Synthesis, liquid crystalline properties and fluorescence of polycatenar 1,3,4-oxadiazole derivatives

Haitao Wang[a], Fenglong Zhang[a], Binglian Bai[a], Peng Zhang[a], Jianhua Shi[a], Dingyi Yu[b], Yunfeng Zhao[b], Yue Wang[b] and Min Li[a]*

[a]*Key Laboratory of Automobile Materials (MOE) & College of Materials Science and Engineering, Jilin University, Changchun 130012, People's Republic of China;* [b]*State Key Laboratory for Supramolecular Structure and Materials & College of Chemistry, Jilin University, Changchun 130012, People's Republic of China*

(Received 15 March 2008; final form 9 June 2008)

A series of hexacatenar liquid crystals containing the 1,3,4-oxadiazole group as rigid core, i.e. 1,4-bis[(3,4,5-trialkoxyphenyl)-1,3,4-oxadiazolyl]- benzene (P-P-oxd-*n*), were designed and synthesised. Based on a detailed study of their thermotropic phase behaviour and mesophase structures, it was revealed that columnar phases are generated in these materials. Furthermore, combination of experimental and calculated results enabled a proposal for the molecular packing in the mesophase. The photoluminescent properties of these materials were examined using P-P-oxd-8 as an example. A strong blue light emission (λ_{max}=456 nm) was observed in P-P-oxd-8 and a higher quantum yield was obtained in dilute chloroform solution.

Keywords: polycatenar liquid crystals; columnar mesophase; fluorescence; 1,3,4-oxadiazole derivatives

1. Introduction

Organic semiconductors (*1*), which benefit from a unique set of characteristics that combine the electrical properties of (semi)conductors with the properties of plastics, i.e. low cost, versatility of chemical synthesis, ease of processing and flexibility, have extensive applications in organic light-emitting diodes (OLEDs) (*2*), field-effect transistors (OFETs) (*3*), plastic solar cells (*4*) and (bio)chemical sensors (*5*). However, there are still a number of important questions concerning the performance of these organic π-conjugated materials, such as crystal grain boundaries and low charge mobility (*6*). In contrast, liquid crystals, which exhibit high carrier conduction in their mesophases without the need to consider boundary effects, are recognised as a new type of quality organic semiconductor (*7*). In fact, carrier mobilities of $0.1\,cm^2\,V^{-1}\,s^{-1}$ and $1.3\,cm^2\,V^{-1}\,s^{-1}$, respectively, have been measured by pulse-radiolysis time-resolved microwave conductivity (PR-TRMC) for thiophene-based smectic liquid crystals (*7b*) and by the steady-state space-charge limited current (SCLC) technique for columnar perylene diimide (*8*) at ambient temperature.

Among these mesophases, the columnar phase, formed by discotic aromatic mesogens stacking into columns, can be thought of as one-dimensional conducting wires as a result of its unique structure. Since the core–core separation in a columnar mesophase is usually of the order of 3.5 Å, an overlap of the π–π* LUMOs (lowest unoccupied molecular orbitals) should be possible. This would lead to a conduction band for charge transport along the column axis, whereas the insulating flexible long aliphatic chains surround the core and separate the columns from each other (*9*). Polycatenar mesogens, which consist of a long rod-like core ending in two half-disc moieties, provide a new molecular architecture for generating columnar mesophases (*10*). These mesogens also give rise of a missing link between the calamitic and discotic liquid crystals, especially in the case of bi-forked mesogens, which may exhibit nematic (N), lamellar, cubic and columnar mesophases in the same series or in a pure compound (*10*). As a result, much effort has been spent on polycatenar liquid crystals in terms of both basic scientific research and potential applications (*10, 11*).

High-mobility n-type organic semiconductors are a particular requirement for the realisation of the benefits of complementary circuit design, owing to the fact that they are somewhat rare and exhibit poor performance compared with p-type semiconductors (*6b, 12*). Due to the electron-deficient nature of the oxadiazole moiety, their high photoluminescence quantum yield and good thermal and chemical stabilities, aromatically substituted 1,3,4-oxadiazole derivatives have found extensive application as emitting layers or electron transport materials in OLEDs and/or n-type OFETs (*12, 13*). However,

*Corresponding author. Email: minli@mail.jlu.edu.cn

ISSN 0267-8292 print/ISSN 1366-5855 online

DOI: 10.1080/02678290802262737
http://www.informaworld.com

most of the reported 1,3,4-oxadizole derivatives are non-mesomorphic or just show calamitic liquid crystal phases (*14*), with only a few examples of a columnar phase (*15*).

In this paper, a new series of polycatenar molecules is reported that contain the 1,3,4-oxadizole group, i.e. 1,4-bis[(3,4,5-trialkoxyphenyl)-1,3,4-oxadiazolyl]benzene (P-P-oxd-*n*, Scheme 1). Special attention was paid to the thermotropic phase behaviour, mesophase structure and fluorescence of the new compounds. Compared with previous work (*15c*), just one phenyl ring was inserted into the bi-oxadiazole group of 2,2′-bis(3,4,5-trialkoxyphenyl)-bi-1,3,4-oxadiazole (BOXD-T*n*). However, it was found that the Col_L phase of BOXD-T*n* was depressed, whereas the Col_r/Col_h phase was stabilised and, due to the elongation of π-conjugation, an obvious red-shift was observed in both absorption and fluorescent spectra. Interestingly, Park *et al.* reported a compound related to P-P-oxd-12 with two additional $-OH$ group at the central benzene ring; similar molecular packing in the columnar phase was revealed and a remarkable red-shift was observed in both the absorption and fluorescent spectra, which was contributed to the enhancement of the planarity and the partial elongation of π-conjugation that results from its strong intramolecular hydrogen bonding (*15e*).

2. Experimental

Synthesis

The synthesis of P-P-oxd-*n* is similar to their mono-substituted analogues, 1,4-bis[(4-alkoxyphenyl)-1,3,4-oxadiazolyl]benzene (OXD_{3-n}, Scheme 1). A detailed description of the synthesis and purification of intermediate compounds can be found elsewhere (*16*). The target oxadiazole derivatives were purified by repeated recrystallisation from tetrahydrofuran (yield >40%) before further ^{1}H NMR and FT-IR measurements and elemental analysis.

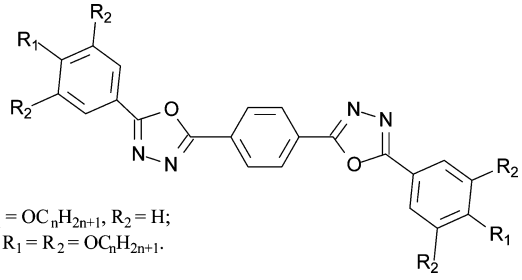

OXD_{3-n}: $R_1 = OC_nH_{2n+1}$, $R_2 = H$;
P-P-oxd-*n*: $R_1 = R_2 = OC_nH_{2n+1}$.

Scheme 1. The molecular structures of OXD_{3-n} and P-P-oxd-*n*.

1,4-bis[(3,4,5-trioctyloxyphenyl)-1,3,4-oxadiazolyl] benzene (P-P-oxd-8)

^{1}H NMR (500 MHz, $CDCl_3$): δ 8.24 (s, 4H); 7.27 (s, 4H), 4.03 (t, 8H, J=6.4 Hz), 3.99 (t, 4H, J=6.6 Hz), 1.80 (m, 8H); 1.71 (m, 4H), 1.44 (m, 12H), 1.35–1.17 (m, 48H), 0.82 (t, 18H, J=6.31 Hz). FT-IR (KBr disk, cm^{-1}): 3437, 2922, 2853, 1593, 1546, 1490, 1438, 1386, 1323, 1237, 1118, 1016, 987, 872, 847, 787, 727, 670, 603. Elemental analysis: calculated for $C_{70}H_{110}N_4O_8$, C 74.03, N 4.93, H 9.76; found, C 74.13, N 4.90, H 10.05%.

1,4-bis[(3,4,5-tridecyloxyphenyl)-1,3,4-oxadiazolyl] benzene (P-P-oxd-10)

^{1}H NMR (500 MHz, $CDCl_3$): δ 8.34 (s, 4H), 7.37 (s, 4H), 4.12 (t, 8H, J=6.5 Hz), 4.08 (t, 4H, J=6.6 Hz), 1.89 (m, 8H), 1.80 (m, 4H), 1.53 (m, 12H), 1.44–1.24 (m, 72H), 0.91 (t, 18H, J=6.78 Hz). FT-IR (KBr disk, cm^{-1}): 3436, 2922, 2850, 1593, 1546, 1488, 1439, 1389, 1324, 1238, 1210, 1119, 1016, 847, 788, 728, 699. Elemental analysis: calculated for $C_{82}H_{134}N_4O_8$, C 75.53, N 4.30, H 10.36; found, C 75.70, N 4.34, H 10.59%.

1,4-bis[(3,4,5-tridodecyloxyphenyl)-1,3,4-oxadiazolyl] benzene (P-P-oxd-12)

^{1}H NMR (500 MHz, $CDCl_3$): δ 8.34 (s, 4H), 7.37 (s, 4H), 4.12 (t, 8H, J=6.4 Hz), 4.08 (t, 4H, J=6.5 Hz), 1.89 (m, 8H), 1.80 (m, 4H), 1.53 (m, 12H), 1.44–1.25 (m, 96H), 0.91 (t, 18H, J=6.9 Hz). FT-IR (KBr disk, cm^{-1}): 3437, 2922, 2849, 1591, 1547, 1468, 1433, 1388, 1324, 1239, 1017, 847, 786, 728, 670. Elemental analysis: calculated for $C_{94}H_{158}N_4O_8$, C 76.68, N 3.81, H 10.82; found, C 76.61, N 3.58, H 11.13%.

1,4-bis[(3,4,5-tritetradecyloxyphenyl)-1,3,4-oxadiazolyl] benzene (P-P-oxd-14)

^{1}H NMR (500 MHz, $CDCl_3$): δ 8.34 (s, 4H), 7.37 (s, 4H), 4.12 (t, 8H, J=6.4 Hz), 4.08 (t, 4H, J=6.5 Hz), 1.89 (m, 8H), 1.80 (m, 4H), 1.53 (m, 12H), 1.45–1.23 (m, 120H), 0.90 (t, 18H, J=6.8 Hz). FT-IR (KBr disk, cm^{-1}): 3437, 2921, 2850, 1593, 1547, 1469, 1434, 1387, 1324, 1239, 1123, 1016, 848, 787, 728. Elemental analysis: calculated for $C_{106}H_{182}N_4O_8$, C77.60, N 3.41, H 11.18; found, C 77.91, N 3.18, H 11.44%.

1,4-bis[(3,4,5-trihexadecyloxyphenyl)-1,3,4-oxadiazolyl] benzene (P-P-oxd-16)

^{1}H NMR (500 MHz, $CDCl_3$): δ 8.34 (s, 4H); 7.37 (s, 4H), 4.12 (t, 8H, J=6.4 Hz), 4.08 (t, 4H, J=6.5 Hz),

1.89 (m, 8H), 1.80 (m, 4H), 1.53 (m, 12H), 1.45–1.23 (m, 144H), 0.90 (t, 18H, J=6.8 Hz). FT-IR (KBr disk, cm^{-1}): 3437, 2921, 2850, 1593, 1547, 1469, 1434, 1387, 1324, 1239, 1123, 1016, 848, 787, 728. Elemental analysis: calculated for $C_{118}H_{206}N_4O_8$, C78.35, N 3.10, H 11.48; found, C 78.13, N 2.86, H 11.54%.

Characterisation

^{1}H NMR spectra were recorded using a Bruker Avance 500MHz spectrometer, with DMSO-d_6 as solvent and tetramethylsilane (TMS) as an internal standard. FT-IR spectra were recorded with a Perkin-Elmer spectrometer (Spectrum One B). Phase transitional properties were investigated using differential scanning calorimetry (Mettler Star DSC 821^e) with heating and cooling rates of 10°C min^{-1}. Texture observation was conducted on a Leica DMLP polarising optical microscope equipped with a Leitz 350 microscope heating stage. X-ray diffraction (XRD) was carried out with a Bruker Avance D8 X-ray diffractometer. Absorption spectra were obtained using a PE UV-vis Lambda 20 spectrometer. Photoluminescence spectra were collected by a Shimadzu RF-5301PC spectrophotometer. The room-temperature luminescence quantum yields were measured at a single excitation wavelength (345 nm) referenced to quinine sulfate in sulfuric acid aqueous solution (0.546), and calculated according to the following equation: $\Phi_{unk}=\Phi_{std}(I_{unk}/A_{unk})(A_{std}/I_{std})(\eta_{unk}/\eta_{std})^2$, where Φ_{unk} is the radiative quantum yield of the sample, Φ_{std} is the radiative quantum yield of the standard, I_{unk} and I_{std} are the integrated emission intensities of the sample and standard, respectively, A_{unk} and A_{std} are the absorptions of the sample and standard at the excitation wavelength, respectively, and η_{unk} and η_{std} are the indexes of refraction of the sample and standard solutions (pure solvents were assumed), respectively.

3. Results and discussion

Phase behaviour

The phase behaviours of P-P-oxd-*n* were studied by polarising optical microscopy (POM) and DSC. All of the new compounds exhibit an enantiotropic columnar phase, except P-P-oxd-8, which is non-mesomorphic. Figure 1(a) shows the pseudo focal conic fan-shaped texture of P-P-oxd-14 in its Col_r phase. Additionally, in P-P-oxd-16, apart from columnar phase, another nematic phase above the columnar phase was assigned based on the texture (Figure 1(b)) and X-ray diffraction

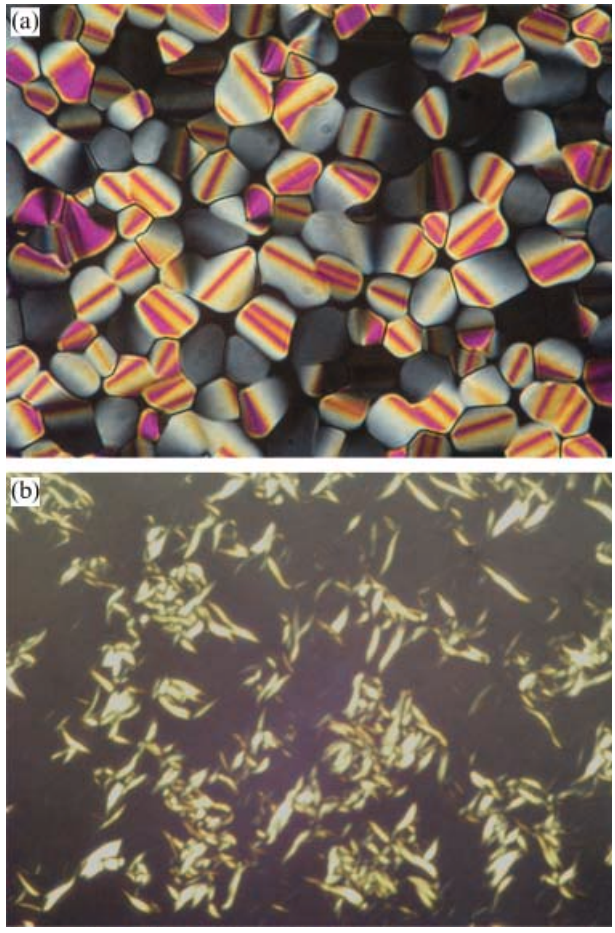

Figure 1. Polarised optical photomicrograph of (a) P-P-oxd-14 in the Col_r phase and (b) P-P-oxd-16 in the nematic phase.

results, in which diffuse peaks were observed in both of the lower and higher angle regions.

Phase transitional temperatures and associated enthalpy changes are summarised in Table 1. It can be seen that the temperature of isotropic transition increases when the number of carbon atoms in the chains varies from 10 to 16 and, thus the mesophase is stabilised by elongating the terminal chain.

Mesophase structures

In order to obtain further information on molecular arrangements in their mesophases, variable

Table 1. Thermotropic phase behaviour of P-P-oxd-*n*.

n	Phase transitions/°C (ΔH/kJ mol^{-1})
8	Cr 103.6 (39.4) I
10	Cr_1 59.2 (37.7) Cr_2 74.8 (55.4) Col_r 80.1 (1.6) I
12	Cr_1 71.7 (65.2) Cr_2 76.8 (65.9) Col_r 81.6 (2.2) I
14	Cr 77.2 (65.9) Col_r 86.5 (2.6) I
16	Cr 64.4 (97.5) Col_h 77.0 (1.3) N 86.5 (0.2) I

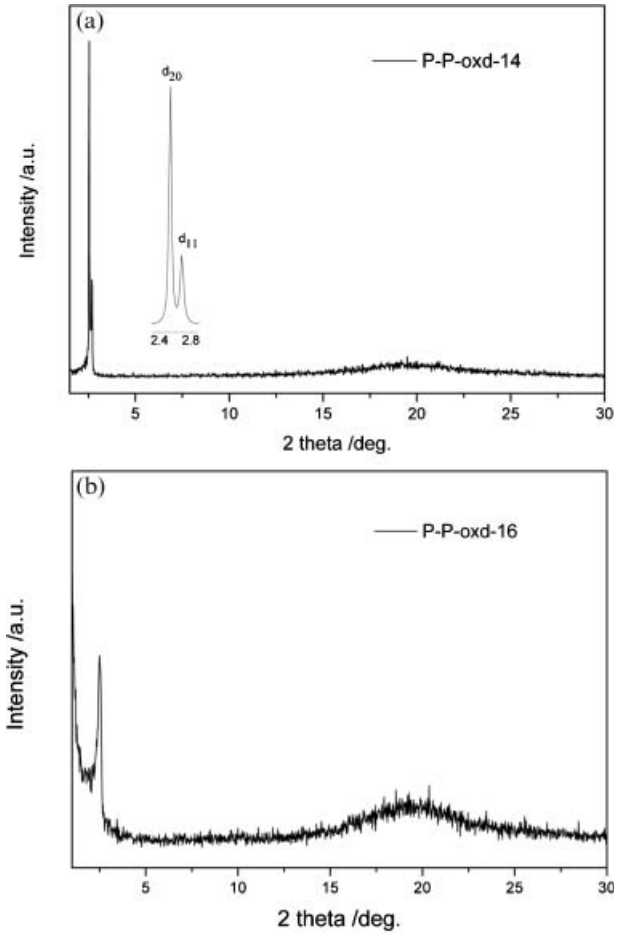

Figure 2. X-ray diffraction patterns of (a) P-P-oxd-14 in the Col_r phase and (b) P-P-oxd-16 in the Col_h phase. The inset in (a) shows the Lorentzian fitted reflection peaks.

temperature X-ray diffraction was performed on these hexacatenar 1,3,4-oxadiazole derivatives.

The columnar rectangular phase (Col_r)

P-P-oxd-12 and P-P-oxd-14 were found to exhibit a columnar phase with rectangular symmetry. As shown in Figure 2(a) for P-P-oxd-14 at 70°C, two intense peaks at d=34.9 Å and d=32.9 Å, and a broad, diffuse halo at about d=4.5 Å were observed. The peaks in the small-angle region correspond to (20) and (11) reflections, respectively, indicating a two-dimensional rectangular arrangement of the columns with lattice parameters of a_r=69.8 Å and b_r=37.3 Å. The scattering halo at high angles ($2\theta \approx 20°$) relates to the liquid-like order of the aliphatic chains. Similar results were obtained for P-P-oxd-12, and the lattice parameters were a_r=61.6 Å and b_r=35.0 Å at 65°C. However, since the higher order reflections are absent, it is not possible to discriminate between the symmetries of columnar rectangular phase, i.e. between the *c2mm* and *p2gg* planar groups (*17*).

Table 2. Lattice parameters of Col_r and Col_h phases for P-P-oxd-*n*.

			Lattice parameters/Å		
n	Phase	*T*/°C	a_r (*a*)	b_r	a_r/b_r
12	Col_r	75	61.2	34.4	1.78
		70	61.4	34.7	1.77
		65	61.6	35.0	1.76
		60	62.2	35.3	1.76
		55	62.6	35.5	1.76
		50	63.0	35.8	1.76
14	Col_r	85	67.8	36.3	1.87
		81	68.0	36.7	1.85
		77	69.0	36.8	1.88
		70	69.8	37.3	1.87
		60	71.2	37.8	1.88
		50	72.8	38.7	1.88
16	Col_h	70	40.6	—	—
		68	41.1	—	—
		65	41.3	—	—

The columnar hexagonal phase (Col_h)

P-P-oxd-16 exhibits a columnar phase with hexagonal symmetry (*p6mm*). As shown in Figure 2(b), at 70°C only one sharp peak at d=35.2 Å and a broad, diffuse halo at about d=4.5 Å were observed. The peak in the small-angle region was assigned to a (10) reflection, indicating a two-dimensional hexagonal arrangement of the columns with a lattice parameter of a=40.6 Å.

Variation of structural parameters with chain length and temperatures

The variation in the lattice parameters as a function of chain length and temperature for P-P-oxd-*n* is summarised in Table 2 and Figure 3. As can be seen, for all the materials the lattice parameter is slightly temperature-dependent; it becomes smaller as the temperature increases. The b_r values in the columnar rectangular phase of P-P-oxd-12 and P-P-oxd-14 are comparative to the a parameter in the hexagonal columnar phase of P-P-oxd-16 and there is an expected monotropic increase in the lattice parameters as the chain length increases. These observations indicate that the transition from the columnar rectangular phase to the hexagonal phase by increasing the chain length is continuous, and the molecular packing in the two phases should be similar. Moreover, in the rectangular columnar phase of both P-P-oxd-12 and P-P-oxd-14, the a_r/b_r ratio is larger than $\sqrt{3}$, indicating that the formation

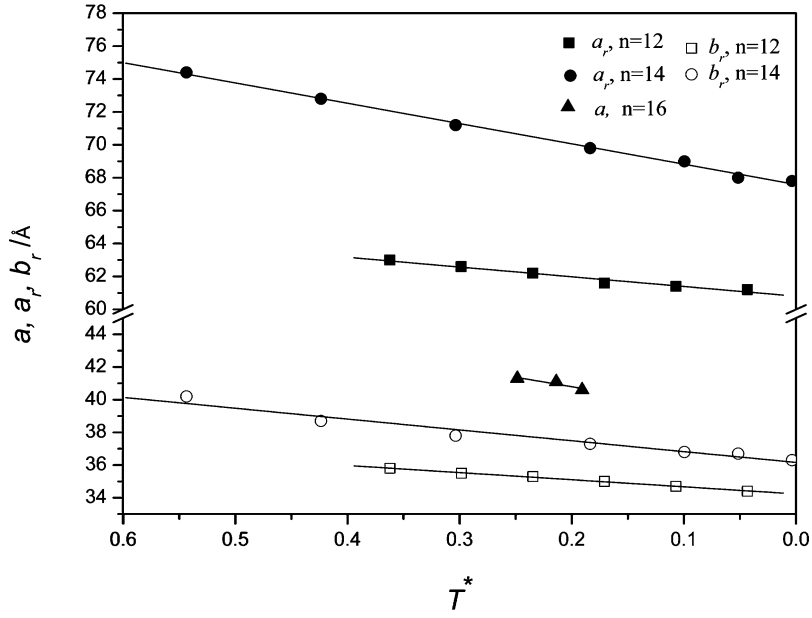

Figure 3. Variation of a_r, b_r and a with T^* ($T^*=1-T/T_i$) of the columnar phases.

of the rectangular networks might be induced by an elongation in the a_r direction.

This supposition can be further confirmed by the analysis of the variation of the columnar area, s, shown in Figure 4. This reveals a monotonic increase with the elongation chain, but both of the rectangular columnar phase and the hexagonal phase are in the same range of 1000~1500 Å^2, suggesting that the columnar section may contain the same number of molecules in these columnar slices. This finding agrees well with the calculation described below.

Molecular packing in the columnar phase

With these data in hand, it is possible to obtain some ideas of the molecular packing in the columns. First, the average number of molecules (μ) in a column slice can be calculated through the equation $\mu=(N_A a_r b_r h\rho)/2M$ for rectangular columnar phase and

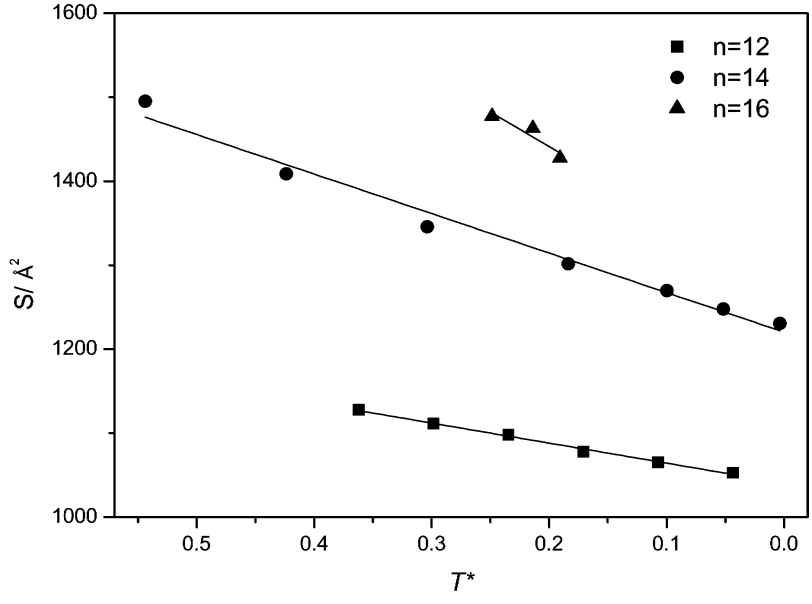

Figure 4. Variation of columnar area, s, with T^* ($T^*=1-T/T_i$) of the columnar phases.

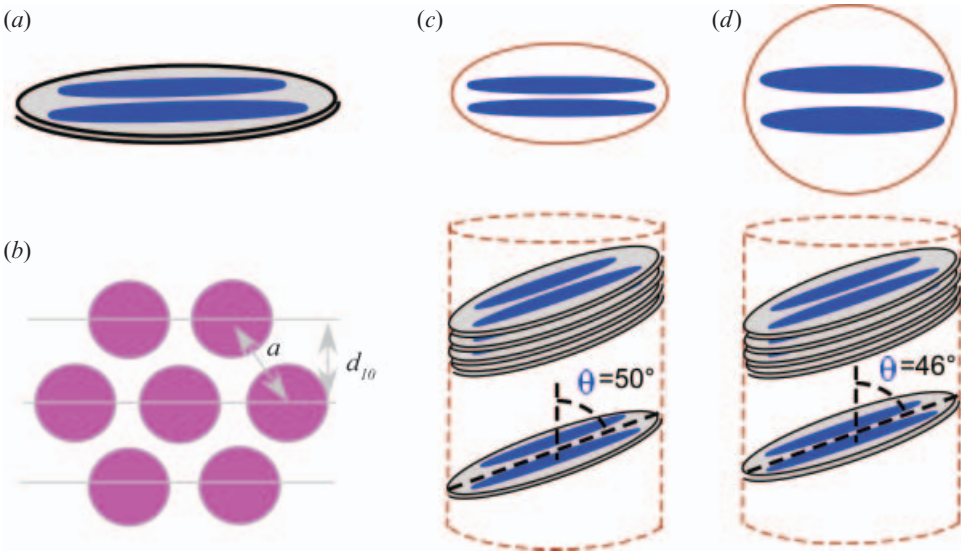

Figure 5. Schematic molecular stacking in the columns: (a) illustration of two molecules per columnar slice; (b) columnar hexagonal arrangement; (c) elliptical-shaped cross-section formed in Col_r phase; (d) circular-shaped cross-section formed in Col_h phase.

$\mu=(\sqrt{3}N_A a^2 h\rho)/2M$ for the hexagonal, where N_A is Avogadro's number, a_r, b_r and a are lattice parameters, h is the intracolumnar periodicity [estimated as ca. 3.8–4.5 Å based on the X-ray crystal structures of 1,3,4-oxadiazole derivatives (*18*)], ρ is the density (assumed to be $1\,g\,cm^{-3}$) and M is the molecular weight of the compound (*19*). For these materials, it can be estimated that approximately two molecules (1.8–2.1, as calculated) are included in a unit slice on average (Figure 5(a)). Also, μ can be proposed from a geometric relationship between the length of the hard core, l, and μ. By assuming that the rigid part of the column defines a circular cross-section of a diameter l, then its circumference must be πl. Further, each chain that radiates from, or crosses, that circumstance (i.e. the core–chain interface) is assumed to require about 5.1 Å (*19*). Thus, the number of chains that can be accommodated in the circular cross-section is $(\pi l)/5.1=12.9$ (where l was evaluated as 21 Å). As we have six chains in each molecule, so there are also about two molecules per columnar slice (Figure 5(a)).

It should be noted that the intercolumnar distance of these oxadiazole derivatives is much smaller than the fully extended molecular length (calculated by MM2), which may indicate that the hexacatenar

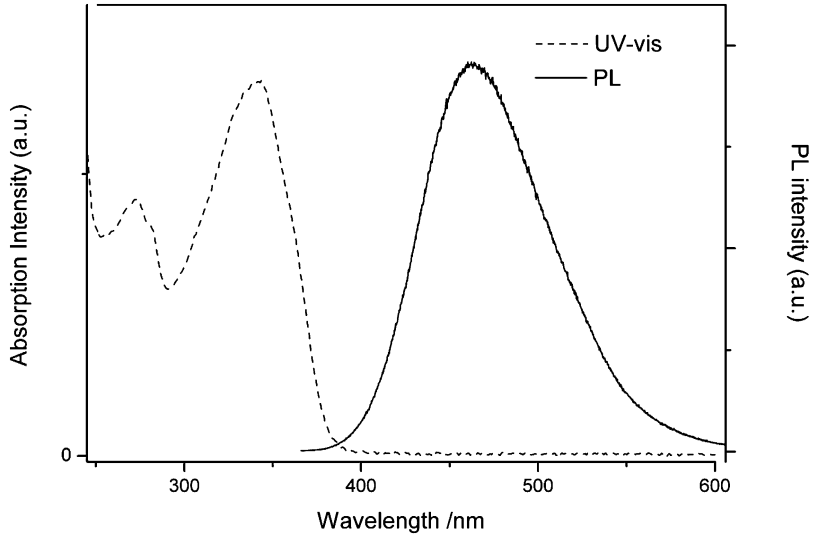

Figure 6. UV–visible absorption (dashed line) and PL spectra (solid line) of P-P-oxd-8 in chloroform (5×10^{-6} M).

molecules are tilted with respect to the cross-section of each column. It is also reasonable to consider it to be tilted if you notice that an ellipse is formed by the two hexacatenar molecules. Also, from the longitudinal offset, the tilted stacking angle (θ) in the columns is estimated to be 50° in the Col_r phase of P-P-oxd-12 and P-P-oxd-14 (*c2mm* group assumed) and 46° in the Col_h phase of P-P-oxd-16 with respect to the columnar axis, under the ideal condition that no interdigitation is considered. Similar structures have already been reported for polycatenar mesogens (*15e, 20*). It seems, therefore, that the core of the column is composed of rigid-rod aromatic benzene-oxadiazole conjugated groups and they are separated by flexible alkoxy chains to form rectangular or hexagonal symmetry. The microphase segregation between the rigid-rod core and the flexible chains, the π–π stacking between the π-conjugated central moieties, as well as efficient filling of the space are responsible for this self-assembling process.

Photoluminescence (PL)

P-P-oxd-8 was taken as an example to test the photoluminescent properties of these materials. Figure 6 shows the UV–visible absorption and PL spectra of P-P-oxd-8 in chloroform (5×10^{-6} M). It can be seen that the absorption maxima occur at about 270 and 340 nm; according to the experimental and calculated results reported previously the main peak should be assigned to π–π* transitions (*16, 21*). The PL spectra, which were recorded in chloroform solution with an excitation at 345 nm, showed a maximum at 456 nm. The maxima of both the absorption and photoluminescence of P-P-oxd-8 are almost concentration-independent in the concentration range from 10^{-4} to 10^{-6} M; the maximum of absorption remained almost constant, whereas the PL maximum underwent a shift of only about 5 nm. However, the intensity is much more concentration-dependent; it decreased with the increase of concentration due to the concentration quenching. Thus, the quantum yield was measured to change from 93% (5×10^{-6} M) to 30% (1×10^{-4} M) on increasing the concentration.

4. Conclusion

P-P-oxd-*n* exhibit columnar mesophases and the symmetry of the mesophase changes from rectangular to hexagonal on increasing the length of the alkoxy chains. A detailed X-ray diffraction study suggests that each columnar slice should consist of two hexacatenar oxadiazole molecules with a tilt angle of 50° in the Col_r phase and 46° in the Col_h phase with respect to the columnar axis. The driving force for the columnar phase was considered to be microphase segregation between the rigid-rod core and the flexible chains, the π–π stacking between the π-conjugated central aromatically substituted oxadiazole groups as well as efficient filling of the space. Moreover, these materials exhibit good photoluminescent properties, as strong blue light emission ($\lambda_{max=}$456 nm) was observed in P-P-oxd-8 and high quantum yield was obtained in dilute chloroform solution. In conclusion, photo-electronic active polycatenar liquid crystalline 1,3,4-oxadiazole derivatives have been synthesised. The combination of liquid crystalline and semiconducting properties may lead to their potential application as high charge mobility materials and further research is in progress.

Acknowledgement

Haitao Wang would like to thank Dr. Renfan Shao and Arthur Klittnick for helpful discussions. This work was supported by Program for New Century Excellent Talents in Universities of China Ministry of Education, Special Foundation for PhD Program in Universities of China (MOE, Project No. 20050183057), Project 985-Automotive Engineering of Jilin University, and the State Scholarship Fund from the China Scholarship Council.

References

(1) Brutting W (Ed.). *Physics of Organic Semiconductors*; Weinheim: Wiley-VCH Verlag, 2005.

(2) (a) Tang C.W.; VanSlyke S.A. *Appl. Phys. Lett.* **1987**, *51*, 913–915; (b) Burroughes, J.H.; Bradley, D.D.C.; Brown, A.R.; Marks, R.N.; Friend, R.H.; Burn, P.L.; Holmes, A.B. *Nature* **1990,** *347,* 539–541.

(3) (a) Horowitz G. *Adv. Mater.* **1998**, *10*, 365–377; (b) Koezuka, H.; Tsumura, A.; Ando, T. *Synth. Meth.* **1987,** *18,* 699–704; (c) Garnier, F.; Hajlaoui, R.; Yassar, A. *Science* **1994,** *265,* 1684–1686; (d) Drury, C.J.; Mutsaers, C.M.J.; Hart, C.M.; Matters, M.; de Leeuw, D.M. *Appl. Phys. Lett.* **1998,** *73,* 108–110; (e) van Breemen, A.J.J.M.; Herwig, P.T.; Chlon, C.H.T.; Sweelssen, J.; Schoo, H.F.M.; Setayesh, S.; Hardeman, W.M.; Martin, C.A.; de Leeuw, D.M.; Valeton, J.J.P.; et al. *J. Am. Chem. Soc.* **2006,** *128,* 2336–2345.

(4) (a) Halls J.J.M.; Walsh C.A.; Greenham N.C.; Marseglia E.A.; Friend R.H.; Moratti S.C.; Holmes A.B.. *Nature* **1995**, *376*, 498–500; (b) Brabec, C.J.; Sariciftci, N.S.; Hummelen, J.C. *Adv. Funct. Mater.* **2001,** *11,* 15–26.

(5) (a) Zhou Q.; Swager T.M. *J. Am. Chem. Soc.* **1995**, *117*, 12593–12602; (b) McQuade, D.T.; Pullen, A.E.; Swager, T.M. *Chem. Rev.* **2000,** *100,* 2537–2574; (c) McQuade, D.T.; Hegedus, A.H.; Swager, T.M. *J. Am. Chem. Soc.* **2000,** *122,* 12389–12390.

(6) (a) Katz H.E.; Bao Z. *J. Phys. Chem. B* **2000**, *104*, 671–678; (b) Newman, C.R.; Frisbie, C.D.; da Silva Filho, D.A.; Bredas, J.L.; Ewbank, P.C.; Mann, K.R. *Chem. Mater.* **2004,** *16,* 4436–4451.

(7) (a) O'Neill M.; Kelly S.M. *Adv. Mater.* **2003**, *15*, 1135–1146; (b) Funahashi, M.; Hanna, J.I. *Adv. Mater.* **2005,** *17,* 594–598.
(8) An Z.; Yu J.; Jones S.C.; Barlow S.; Yoo S.; Domercq B.; Prins P.; Siebbeles L.D.A.; Kippelen B.; Marder S.R. *Adv. Mater.* **2005**, *17*, 2580–2583.
(9) (a) Sergeyev S.; Pisula W.; Geerts Y.H. *Chem. Soc. Rev.* **2007**, *36*, 1902–1929; (b) Laschat, S.; Baro, A.; Steinke, N.; Giesselmann, F.; Hagele, C.; Scalia, G.; Judele, R.; Kapatsina, E.; Sauer, S.; Schreivogel, A. et al. *Angew. Chem., Int. Ed.* **2007,** *46,* 4832–4887; (c) Kumar, S. *Chem. Soc. Rev.* **2006,** *35,* 83–109; (d) Adam, D.; Schuhmacher, P.; Simmerer, J.; Haussling, L.; Siemensmeyer, K.; Etzbach, K.H.; Ringsdorf, H.; Haarer, D. *Nature* **1994,** *371,* 141–143.
(10) Nguyen H.T.; Destrade C.; Malthete J. In *Handbook of Liquid Crystals,* Vol. 2B, Demus D., Goodby J., Gray G.W., Spiess H.W., Vill V. (Eds), Weinheim: Wiley-VCH, 1998; 865–885.
(11) Gharbia M.; Gharbi A.; Nguyen H.T.; Malthete J. *Curr. Opin. Colloid Interface Sci.* **2002**, *7*, 312–325.
(12) Thelakkat M.; Schmidt H.-W. *Polym. Adv. Technol.* **1998**, *9*, 429–442.
(13) Schultz B.; Bruma M.; Brehmer L. *Adv. Mater.* **1997**, *9*, 601–613.
(14) (a) Girdziunaite D.; Tschierske C.; Novotna E.; Kresse H.; Hetzheim A. *Liq. Cryst.* **1991**, *10*, 397–407; (b) Schulz, B; Orgzall, I.; Freydank, A.; Xu, C. *Adv. Colloid Interface Sci.* **2005,** *116,* 143–164; (c) Karamysheva, L.; Torgova, S; Agafonova, I.; Petrov, V. *Liq. Cryst.* **2000,** *27,* 393–405.
(15) (a) Zhang Y.D.; Jespersen K.G.; Kempe M.; Kornfield J.A.; Barlow S.; Kippelen B.; Marder S.R. *Langmuir* **2003**, *19*, 6534–6536; (b) Lai, C.K.; Ke, Y.C.; Su, J.C.; Lu, C.S.; Li, W.R. *Liq. Cryst.* **2002,** *29,* 915–920; (c) Qu, S.; Li, M. *Tetrahedron* **2007,** *63,* 12429–12436; (d) He, C.; Richards, G.; Kelly, S; Contoret, A; O'Neill, M. *Liq. Cryst.* **2007,** *34,* 1249–1267; (e) Seo, J.; Kim, S.; Gihm, S.; Park, C.; Park, S. *J. Mater. Chem.* **2007,** *17,* 5052–5057.
(16) Zhang X.; Tang B.; Zhang P.; Li M.; Tian W. *J. Mol. Struct.* **2007**, *642*, 53–62.
(17) Levelut A.M. *J. Chim. Phys.* **1983**, *80*, 149–161.
(18) (a) Schulz B.; Orgzall I.; Freydank A.; Xu C. *Adv. Colloid Interface Sci.* **2005**, *116*, 143–164; (b) Yu, H.; Huang, Y.; Zhang, W.; Matsuura, T.; Meng, J. *J. Mol. Struct.* **2002,** *642,* 53–62.
(19) Guillon D. *Struct. Bonding* **1999**, *95*, 42–82.
(20) (a) Wurthner F.; Thalacker C.; Diele S.; Tschierske C. *Chem. Eur. J.* **2001**, *7*, 2245–2253; (b) Yasuda, T.; Kishimoto, K.; Kato, T. *Chem. Commun.* **2006,** 3399–3401.
(21) Zhang P.; Xia B.; Zhang Q.; Yang B.; Li M.; Zhang G.; Tian W. *Synth. Meth.* **2006**, *156*, 705–713.